[7]V. I. Bespalov and A. M. Kubarev, Zh. Eksperim. i Teor. Fiz. Pis'ma v Redaktsiyu 6, 500 (1967) [Soviet Phys. JETP Letters 6, 31 (1967)].

[8]I. M. Aref'ev and V. V. Morozov, Zh. Eksperim. i Teor. Fiz. Pis'ma v Redaktsiyu 9, 448 (1969) [Soviet Phys. JETP Letters 9, 296 (1969)].

[9]N. Bloembergen, W. H. Lowdermilk, M. Matsuoka, and C. S. Wang, paper presented at the Sixth International Conference on Quantum Electronics, Kyoto, 1970 (unpublished).

[10]See, for example, F. V. Hunt, in *American Institute of Physics Handbook* (McGraw-Hill, New York, 1957); or L. D. Landau and E. M. Lifshitz, *Fluid Mechanics* (Addison-Wesley, Reading, Mass., 1958). We follow the notations of this last reference.

[11]S. Chapman and T. G. Cowling, *Mathematical Theory of Nonuniform Gases* (Cambridge U. P., Cambridge, England, 1952), or J. O. Hirshfelder, C. F. Curtis, and R. B. Bird, *The Molecular Theory of Gases and Liquids* (Wiley, New York, 1954).

[12]S. Yip and M. Nelkin, Phys. Rev. 135, A1241 (1964); N. Clark, Ph. D. thesis, M. I. T., 1970 (unpublished). The parameter y characterizes the transition of the kinetic to the hydrodynamic regime of a single component fluid; the transition between these regimes in a mixture is yet to be investigated. However, one can expect that if one component is in the hydrodynamic regime with its partial pressure the mixture should be in the hydrodynamic regime.

[13]See Refs. 1 and 11.

[14]K. A. Brueckner and S. Jorna, Phys. Rev. Letters 17, 78 (1966); Phys. Rev. 164, 182 (1967); N. M. Kroll and P. L. Kelley (unpublished).

[15]R. M. Herman and M. A. Gray, Phys. Rev. Letters 19, 824 (1967).

[16]See Refs. 5 and 6, and other papers quoted therein.

[17]C. S. Wang, Phys. Rev. Letters 24, 1394 (1970). The additional term was kindly called to our attention by Professor R. M. Herman. The total intensity-dependent shift should be the value given in Eq. (33) plus the value calculated in this reference, i.e., $\Delta\nu_s^2 = -(5\epsilon+2)\times\rho_0(\partial\epsilon/\partial\rho)^2|E_l|^2/16\pi(\epsilon+2)\epsilon$. This makes the agreement with the experimental breakdown intensity even better. For gases with high polarizabilities such as SF_6 and Xe, the intensity-dependent effect is comparatively small. We shall neglect this effect in the following calculations.

[18]M. Kohler, Ann. Physik 39, 209 (1941); this extra damping is also discussed in Ref. 10.

[19]E. E. Hagenlocker, R. W. Minck, and W. G. Rado, Phys. Rev. 154, 226 (1967).

[20]C. L. O'Connor, J. Acoust. Soc. Am. 26, 361 (1954).

PHYSICAL REVIEW A VOLUME 3, NUMBER 1 JANUARY 1971

Phase-Matched Critical Total Reflection and the Goos-Haenchen Shift in Second-Harmonic Generation*

H. Shih and N. Bloembergen†

Division of Engineering and Applied Physics, Harvard University, Cambridge, Massachusetts 02138

(Received 12 August 1970)

It is well established that a totally reflected light beam of finite diameter undergoes a lateral displacement, known as the Goos-Haenchen shift. The theory for the corresponding effect in nonlinear optics is presented. The special phase-matched case, in which both the fundamental and the second harmonic are at critical total reflection, is shown to have a characteristic radiation pattern. Since the finite beam diameter is taken into account, divergencies of earlier theories are eliminated.

I. INTRODUCTION

When a light beam is totally reflected, there is no net power flux normal to the boundary into the less dense medium. There is, however, a nonvanishing component of the Poynting vector tangential to the boundary. The fields decay exponentially normal to the boundary in the less dense medium, but this decay of the evanescent field becomes infinitely slow at the critical angle, for which total reflection first occurs. There is a singularity in $\vec{k}$ space, as the normal component k_z in the less dense medium changes from small positive values through zero to pure imaginary values. An accurate description of the phenomenon of critical total reflection must consider explicitly the finite diameter of the light beam and integrate properly over a distribution in $\vec{k}$ space around the critical point. This problem in linear optics has been discussed by many authors[1] and was solved in a rather complete form by Artman.[2] The field distribution of the fundamental light beam, of width w_0 in the less dense optical medium for critical total reflection, is shown in Fig. 1. The transverse component of the Poynting vector corresponds to a lateral displacement of the reflected beam. This displacement has been observed experimentally and is known as the Goos-Haenchen shift.[3,4]

It is the purpose of this paper to extend these considerations to the domain of nonlinear optics, in particular, to the case of harmonic generation of light by a totally reflected fundamental beam. The theory of total reflection of parametrically generated light has been given by Bloembergen and

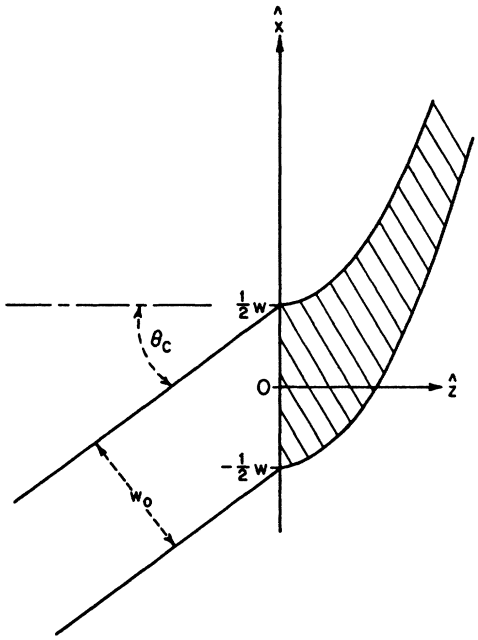

FIG. 1. A light beam of width w_0 is incident on a less dense optical medium, which occupies the half-space $z>0$. The angle of incidence θ_c corresponds to critical total reflection. The field distribution inside the less dense medium is essentially confined to the shaded area, according to Artman (Ref. 2). It is bounded by the parabola $z=[(2x-w)\lambda_2/\pi]^{1/2}$ and $z=[(2x+w)\lambda_2/\pi]^{1/2}$.

Pershan.[5] They treat the case of light beams of infinite cross section, or a δ function in $\vec{k}$ space. This formulation leads to a divergence in the reflected harmonic intensity for the case of phase-matched critical total reflection.

Totally reflected second-harmonic light was first observed by Bloembergen and Lee.[6] Their experimental results for the above-mentioned case are compared with the theory of Bloembergen and Pershan in Fig. 2. Further experimental results were obtained for phase-matched third-harmonic reflection by Bey, Giuliani, and Rabin.[7] Detailed experimental results for the non-phase-matched case of totally reflected second-harmonic generation have also been given. In all these experiments only the total harmonic power in the far field is observed.

In Sec. II of this paper a Green's-function formulation is developed to describe the generated harmonic field, with due attention being paid to the effects of the finite beam diameter. In Sec. III both the near- and far-field distributions for the case of phase-matched critical total reflection (PMCTR) of harmonic generation will be presented. In Sec. IV the nonlinear analog of the spatial Goos-Haenchen shift is calculated for both the phase-matched and mismatched cases of total reflection. This shift of the harmonic reflected radiation should be observable in the near field.

II. GREEN'S FUNCTION FOR THE SECOND-HARMONIC FIELD NEAR CRITICAL TOTAL REFLECTION

The Green's-function technique in harmonic generation has been used previously by Kleinman and collaborators[8,9] to discuss the influence of a finite beam diameter on transmitted second-harmonic radiation near phase matching in uniaxial crystals. It was also applied to conical refraction of second harmonics in biaxial crystals.[10] It is essential to use this technique in the case of PMCTR to handle the singularities in $\vec{k}$ space.

In the parametric approximation, the distribution of the second-harmonic nonlinear source polarization is prescribed in terms of the nonlinear susceptibility tensor of the medium and the distribution of the fundamental field. In the case of critical total fundamental reflection the second-harmonic sources will be confined to a region as depicted in Fig. 1. The phase of the source in each volume element is, of course, determined by the phase of the fundamental field.

The elementary source volume element is chosen as a slab of finite lateral dimensions, large compared to the wavelength in the x and y directions, tangential to the boundary, but infinitesimally small in the normal z direction. This choice ensures that the phase coherence properties giving rise to specular reflection are explicitly exhibited in the Green's function which takes the form[11]

$$G^b=\exp[i\vec{k}_T\cdot(\vec{r}-\vec{r}')-i(\vec{k}_0^{SH}\cdot\hat{z})(z-z')]$$
$$\times\int d\vec{k}_T'\,2\pi(2\omega/c)^2(i\vec{k}^{SH}\cdot\hat{z})^{-1}t_{21}^{SH}$$
$$\times\exp[i\vec{k}_T'\cdot(\vec{r}-\vec{r}')-i\delta k_z^{SH}(z-z')], \qquad (1)$$

where

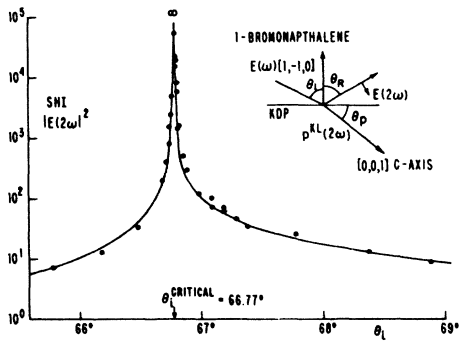

FIG. 2. Integrated second-harmonic power in reflection from a KDP crystal as a function of the angle of incidence, according to Bloembergen and Lee (Ref. 6). Phase matching occurs at the critical total reflection. The drawn curve corresponds to the theory of Bloembergen and Pershan (Ref. 5).

$$\delta k_z^{SH} = (\vec{k}^{SH} - \vec{k}_0^{SH}) \cdot \hat{z},$$

$$\vec{k}_T' = (\vec{k}^{SH} - \vec{k}_0^{SH}) \cdot (\vec{1} - \hat{z}\hat{z}),$$

$$t_{21}^{SH} = 2\vec{k}^{SH} \cdot \hat{z} / (\vec{k}_1^{SH} \cdot \hat{z} + \vec{k}^{SH} \cdot \hat{z}).$$

Here t_{21}^{SH} represents the Fresnel transmission factor at the boundary. The wave vector $\vec{k}^{SH}$ represents a Fourier component in the wave packet of the second harmonic, centered around $\vec{k}_0^{SH}$ which represents the nominal value of the second-harmonic wave in the medium. The deviation from this nominal value for the z component is δk_z^{SH}. The subscript T denotes tangential components.

The reflected harmonic field just outside the boundary at $z = 0$ is given by

$$E^{SH}(\vec{r})|_{z=0} = \int d\vec{r}\,' G^b(\vec{r} - \vec{r}\,') P^{SH}(\vec{r}\,'), \tag{2}$$

where the integration is over the half-space occupied by the nonlinear crystal.

While the Green's function of Eq. (2) is defined in the real $\vec{r}$ space, Eq. (1) shows that G^b itself depends explicitly on $\vec{k}_0^{SH}$, a quantity defined in the transformed $\vec{k}$ space. Our approach is therefore more or less a mixture of the approaches in the $\vec{r}$ and $\vec{k}$ spaces. As we have mentioned, it is necessary to consider a region rather than just a single point $\vec{k}_0^{SH}$ in the $\vec{k}$ space. The $\vec{k}_T'$ integration in Eq. (1) does just that.

Note that the scalar form of Eqs. (1) and (2) deals only with the case where the polarization is perpendicular to the plane of incidence. For simplicity, we also neglect anisotropy of the media. However, it is easy to take into account the anisotropy and more general situations for the polarization.[11]

For SHG close to the region of critical total reflection, we may approximate the variation δk_z^{SH} of the normal z component of the wave vector as a function of the changes $\vec{k}_T'$ in the transverse components as

$$\delta k_z' = [(k^{SH} + k_x^0 + k_x')(k^{SH} - k_x^0 - k_x')]^{1/2} \approx \beta(b - k_x')^{1/2}, \tag{3}$$

where

$$\beta = (k^{SH} + k_x^0)^{1/2} \approx (k^{SH} + k_x^0 + k_x')^{1/2},$$

$$b = k^{SH} - k_x^0, \qquad k_x^0 = \hat{x} \cdot \vec{k}_0^{SH}.$$

In the limiting case of PMCTR, the parameter b equals zero. The xz plane is the plane of incidence. The integration over k_y' in Eq. (1) is trivial, and this expression is reduced to

$$G^b = \xi \exp[ik_x^0 X + i\vec{k}_0^{SH} \cdot \hat{z} Z] \int_{-\infty}^{\infty} dk_x' \times \exp[ik_x' X - iZ\beta(b - k_x')^{1/2}], \tag{4}$$

where

$$\xi = \delta(y - y')2(2\pi)^{3/2}(2\omega/c)^2(i\vec{k}_1^{SH} \cdot \hat{z})^{-1}$$

$$X = x - x', \qquad Z = z - z'.$$

It may equally well be rewritten as a contour integral in the complex p plane with $(b - k_x')$ identified as the real part of p. Thus, we have

$$G^b = \xi\xi' \exp(ik_x^0 X - i\vec{k}_0^{SH} \cdot \hat{z} Z),$$
$$\xi' = \int_C dp \exp(-ipX - i\beta Z p^{1/2}). \tag{5}$$

The contour C is taken along the real axis in the p plane as shown in Fig. 3. Also shown there is the branch cut which makes a small angle δ with the positive real axis. The reason for the choice of the cut will be clear later and δ will be taken in the limit towards zero from the positive side, i.e., $\delta \to +0$.

For negative values of X, i.e., for $x < x'$, the contour of integration may be closed in the upper half-plane by the semicircle C_1. Since the function $\exp(-ipX - i\beta Z p^{1/2})$ is analytic in the upper half-plane, the use of the residue theorem yields

$$0 = (\int_C + \int_{C_1}) dp \exp(-ipX - i\beta Z p^{1/2})$$
$$= \int_{-R}^{R} dr \exp(-irX - i\beta Z r^{1/2}) + \int_{\pi}^{0} d\phi\, R \exp(-iRe^{i\phi}X - i\beta Z R^{1/2} e^{i\phi/2}).$$

The integral along C_1 approaches zero as the contour C_1 tends to infinity, i.e., as $R \to \infty$. We thus conclude that

$$\xi' = \lim_{R\to\infty} \int_{-R}^{R} dr \exp(-irX - i\beta Z r^{1/2}) = 0 \quad \text{for } X < 0. \tag{6}$$

For positive values of X, i.e., for $x > x'$, the

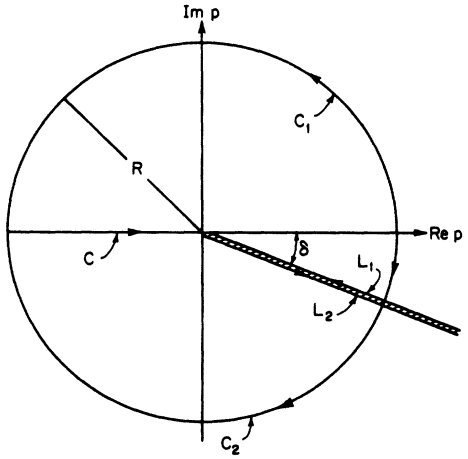

FIG. 3. Paths of contour integrations in the p plane to evaluate the Green's function for PMCTR, given by Eq. (5).

contour of integration may be closed in the lower half-plane by the branch cut are also included. By and L_2 along the branch cut are also included. By inspection of Fig. 3, the residue theorem yields

$$\left(\int_C + \int_{L_1} + \int_{L_2} + \int_{C_2}\right) dp\, e^{-ipx - i\beta z p^{1/2}} = 0.$$

In the limit that the contour C_2 tends to infinity, i.e., $R \to \infty$, and that $\delta \to +0$, the contribution from the contour C_2 vanishes;

$$\begin{aligned}
\xi' &= -\lim_{\delta \to +0} \left(\int_{L_1} + \int_{L_2}\right) dp\, e^{-ipx - i\beta z p^{1/2}} \\
&= -\lim_{\delta \to +0} \left[\int_{\infty}^{0} dr (e^{-i\delta} e^{-ipx - i\beta z p^{1/2}})_{p = re^{-i\delta}} e^{-i\delta} \right. \\
&\quad \left. - \int_{0}^{\infty} dr (e^{-i\delta} e^{-ipx - i\beta z p^{1/2}})_{p = re^{i(2\pi - \delta)}} \right] \\
&= \lim_{\delta \to +0} \int_0^{\infty} dr\, e^{-ixr(1 - i\delta)} (-2i) \sin[\beta z r^{1/2}(1 - i\delta/2)] \\
&= \lim_{\delta \to +0} (-4i) \int_0^{\infty} d\eta\, \eta\, e^{-(i+\delta)x\eta^2} \sin[\beta z \eta (1 - i\delta/2)].
\end{aligned}$$

We have made the change of variable from r to η through the relation $\eta^2 = r$ in the last step.

With the aid of the identity

$$\int_0^{\infty} dx\, x e^{-q^2 x^2} \sin ax = (a\pi^{1/2}/4q^3) e^{-a^2/4q^2} \quad \text{for Re } q^2 > 0,$$

the Green's function for PMCTR takes the form

$$\begin{aligned}
G^b &= 0 \quad \text{for } x - x' < 0 \\
&= \alpha \delta(y - y') [\beta(z - z')/(x - x')^{3/2}] \\
&\quad \times \exp\{i[\beta(z - z')/2(x - x')^{1/2}]^2 \\
&\quad + ik^{SH}(x - x')\} \quad \text{for } x - x' > 0,
\end{aligned} \tag{7}$$

where

$$\alpha = 4\pi(2\omega/c)^2 (i\vec{k}_1^{SH} \cdot \hat{z})^{-1} \pi^{1/2} e^{-i\pi/4}.$$

The physical implication of Eq. (7) has a simple geometrical interpretation. In the case of PMCRT, the relationship $k_x^0 = k^{SH} = k^S$ holds and the field according to Eq. (2) is given by

$$\begin{aligned}
E_{x=0}^{SH} &= \alpha\beta \int_{x > x'} d\vec{r}\, |z - z'| (x - x')^{-3/2} \\
&\quad \times \exp\{i\beta^2 (z - z')^2/4(x - x')\} P^{SH}(\vec{r}\,'),
\end{aligned} \tag{8}$$

where now $P^{SH}(\vec{r}\,')$ is essentially constant, since the phase factor $\exp[-ik^S(x - x')]$ in the source is just cancelled out by the phase factor $\exp[ik^{SH} \times (x - x')]$ of the Green's function. The radiation from different points in the medium may be considered as coherent, if the maximum phase deviation is less than $\pi/2$. This is true for an effective region of radiation bound by the parabola

$$x - x' = (\lambda_2^{SH})^{-1} (z - z')^2$$

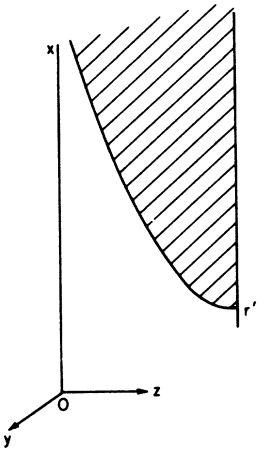

FIG. 4. "Effective region" of radiation from a volume element of SH polarization, located at $\vec{r}\,'$. Outside the shaded region its field is effectively cancelled by contributions from neighboring volume elements. The boundary is given by the $x - x' = (z - z')^2/\lambda_2^{SH}$.

which is shown in Fig. 4. Outside this region the phase in the integrand of Eq. (8) varies rapidly. There will be a cancellation of contributions from neighboring volume elements, at $\vec{r}\,'$ and $\vec{r}\,''$, respectively. The requirement of a "stationary phase" defines an "effective region" of uncancelled contribution of a radiative element at $\vec{r}\,'$, as depicted in Fig. 4.

This argument is essentially the same as that used by Artman in deriving the penetration of the fundamental field at CTR due to sources at the boundary as shown in Fig. 1.

The analytic expression for the transmitted fundamental field is[2]

$$E(x, z) = \int_{-\infty}^{\infty} dx'\, F(x - x', z) \frac{1}{ik_x} \left[\frac{d}{dx'} E(x', z)\right]_{z=0}, \tag{9}$$

where

$$F(x, z) = (2\pi)^{-1} e^{ik_x x} \int d\kappa (i\kappa)^{-1} e^{i\{\kappa x + z[(k_z^0)^2 - (k_x + \kappa)^2]\}^{1/2}}.$$

F is similar to G^b in Eqs. (1) and (5).

In the case of CTR, F is simply

$$F(x - x', z) = \begin{cases} 0 & \text{for } x < x' \\ e^{ik_x^0 (x - x')} e^{i\pi/4} 2\sqrt{2} \int_{-\infty}^{\sigma_c} e^{-i\pi v^2/2} dv & \\ \quad \text{for } x \geq x', & \end{cases} \tag{10}$$

where

$$\sigma_c = -z[k_2^0 \pi/4(x - x')]^{1/2}.$$

It is essentially nonzero only in the region $z \leq [4(x - x')/k_2]^{1/2} = (2/\pi)^{1/2}[\lambda_2 (x - x')]^{1/2}$. This is in agreement with the boundaries shown in Fig. 1.

III. SECOND-HARMONIC FIELD FOR CASE OF PMCTR

A. Near Field

For an incident beam with a uniform intensity in a square cross section the second-harmonic source

polarization

$$P^{SH}(r) = \chi^{NL}E^2(x, z) \tag{11}$$

is confined to the shaded region in Fig. 1. Substitution of Eqs. (9)–(11) and (7) into Eq. (2) yields the following result for the second-harmonic field just outside the nonlinear medium at $z = 0$:

$$E^{SH}_{z=0} = \begin{cases} 0 & \text{for } x < -\frac{1}{2}w \\ \alpha' e^{ik_x^0 x}\,\nu(n')[\lambda_2(x+\frac{1}{2}w)]^{1/2} & \text{for } \frac{1}{2}w > x > -\frac{1}{2}w \\ \alpha' e^{ik_x^0 x}\,\Pi(\xi, n')[\lambda_2(x+\frac{1}{2}w)]^{1/2} & \text{for } x > \frac{1}{2}w, \end{cases} \tag{12}$$

where

$$\nu(n') = \int_0^1 d\zeta\, \zeta^{-3/2} \int_0^\infty d\mu\, \mu\, e^{i2n'\mu^2/\zeta}[\mathcal{E}_f^c(\mu/(1-\zeta)^{1/2})]^2,$$

$$\Pi(\xi, n') = \int_0^{1-\xi} d\zeta\, \zeta^{-3/2} \int_0^\infty d\mu\, \mu\, e^{i2n'\mu^2/\zeta} \times [\mathcal{E}(\mu/(1-\zeta)^{1/2}) - \mathcal{E}_f(\mu/(1-\zeta-\xi)^{1/2})]^2 + \int_{1-\xi}^1 d\zeta\, \zeta^{-3/2} \times \int_0^\infty d\mu\, \mu\, e^{i2n'\mu^2/\zeta}[\mathcal{E}_f^c(\mu/(1-\zeta)^{1/2})]^2,$$

$$\xi = w/(x + \tfrac{1}{2}w),$$

$$n' = \lambda_2/\lambda_2^{SH} = n_2^{SH}/n_2.$$

We have neglected the trivial y dependence here.

The nonlinear susceptibility and transmission factor are absorbed in the proportionality constant α'. The function $\mathcal{E}_f^c(x)$ is related to the Fresnel-diffraction integrals defined by

$$\mathcal{E}_f^c(x) = (1+i)/2 - \mathcal{E}_f(x),$$

$$\mathcal{E}_f(x) = C(x) + iS(x),$$

$$C(x) = \int_0^x dt \cos(\tfrac{1}{2}\pi t^2),$$

$$S(x) = \int_0^x dt \sin(\tfrac{1}{2}\pi t^2).$$

Near the edge at $x = -\frac{1}{2}w$ the field strength increases parabolically as $(x + \frac{1}{2}w)^{1/2}$. This fast rise will, of course, be less abrupt for a more realistic Gaussian-beam profile. But the other features are not changed very much for a Gaussian profile. Beyond the point $x = \frac{1}{2}w$, the field amplitude drops off rather abruptly, but does not vanish. For large value of x the amplitude drops as $x^{-3/2}$.

The analytical expressions Eq. (12) may be simplified somewhat by assuming an effective rectangular source region, with a characteristic penetration depth $l = (\lambda_0^{SH}w)^{1/2} = (\lambda_0^{SH}w_0/\cos\theta_c)^{1/2}$. This value follows from a simple consideration of the diffraction problem. The diffraction limited incident beam of width w_0 causes a spread in the tangential component of the wave vector $\Delta k_x \sim k_1(\lambda_1/w)\cos\theta_c$. Near the angle for CTR this leads to an imaginary part in k_z equal to l^{-1} with a source distribution

$$P^{SH}(\vec{r}) = P_0 e^{-z/l} \text{ for } \begin{cases} -\frac{1}{2}w < x < +\frac{1}{2}w \\ -\frac{1}{2}w_0 < y < +\frac{1}{2}w_0, \end{cases}$$

$$P^{SH}(\vec{r}) = 0 \qquad \text{elsewhere.}$$

The harmonic field just outside the boundary may be evaluated in the form

for $x < -\frac{1}{2}w$,

$$E^{SH}_{z=0} = 0; \tag{13a}$$

for $\frac{1}{2}w > x > -\frac{1}{2}w$,

$$E^{SH}_{z=0} = \alpha_p \beta l^2 \int_0^{x+1/2w} dx''(x'')^{-3/2} \times [1 + (1 + (\lambda_2^{SH}x'')^{1/2}/l)e^{-(\lambda_2^{SH}x'')^{1/2}/l}]$$

$$= \alpha_p(4\pi)^{1/2}2l(\tau_+')^{-1}(e^{-\tau_+'} - 1 + \tau_+'), \tag{13b}$$

where

$$\alpha_p = -i\alpha P_0, \qquad \tau_+' = l^{-1}[\lambda_2^{SH}(x + \tfrac{1}{2}w)]^{1/2} = \left(\frac{x/w + \frac{1}{2}}{n'}\right)^{1/2};$$

and for $x > \frac{1}{2}w$,

$$E^{SH}_{z=0} = \alpha_p(4\pi)^{1/2}2l[(e^{-\tau_+'} - 1)/\tau_+' - (e^{-\tau_-'} - 1)/\tau_-'], \tag{13c}$$

where

$$\tau_-' = \left(\frac{x/w - \frac{1}{2}}{n'}\right)^{1/2}.$$

This form is more convenient for analytic calculations, but the qualitative features of the spatial distribution of the near field remain the same as given by Eq. (12). The numerical result is plotted in Fig. 5.

B. Far Field

From the SH field at the boundary we can obtain the reflected second harmonics at an arbitrary point $\vec{r}$ in the incident medium by use of diffraction theory[12] as follows:

$$\vec{E}_1^{SH}(\vec{r})\,|_{z<0} = -i(\lambda_0^{SH})^{-1} \int d\vec{r}_T' |\vec{r} - \vec{r}'|^{-1} \times e^{i2\pi|r-r'|/\lambda_1^{SH}} \vec{E}^{SH}_{z=0}(\vec{r}'). \tag{14}$$

In the far-field region $|\vec{r} - \vec{r}'| \gg (\lambda_1^{SH}w)^{1/2}$, we may speak of Fraunhofer diffraction. The above expression may then be approximated as[12]

$$\lim_{\substack{Z\to\infty \\ \hat{z}\cdot\hat{r}\to 1}} \vec{E}_1^{SH}(\vec{r})\,|_{z<0} \sim \left(\frac{-i}{\lambda_0^{SH}}\right) e^{i2\pi Z/\lambda_1^{SH}} \frac{1}{Z} \vec{U}(\Theta_X, \Theta_Y), \tag{15}$$

$$\vec{U}(\Theta_X, \Theta_Y) = \int\int dX'dY' e^{i(\Theta_X X' + \Theta_Y Y')2\pi/\lambda_1^{SH}} \vec{E}_1'(X', Y'), \tag{16}$$

where

$$\Theta_X = X/Z,$$

$$\Theta_Y = Y/Z,$$

$$\vec{E}_1'(X, Y) = e^{-ik_x x'}\vec{E}^{SH} \quad (x = X/\cos\theta_1^{SH},\ y = Y,\ z = 0)\ .$$

We have expressed the physical quantities in terms of the new set of coordinates X, Y, Z which is related to the old set of x, y, z by

$$\begin{aligned} X &= x\cos\theta_1^{SH} + z\sin\theta_1^{SH}, \\ Y &= y, \\ Z &= -x\sin\theta_1^{SH} - z\cos\theta_1^{SH}. \end{aligned} \tag{17}$$

For the discussion of the far-field pattern we may focus our attention on the function U which is essentially just the Fourier transform of the field E^{SH} at the boundary.

Combining Eqs. (13), and (15)–(17), we find the following expression for U for the square-beam case:

$$U(\Theta_X, \Theta_Y) = U_X(\Theta_X)\, U_Y(\Theta_Y), \tag{18}$$

where

$$\begin{aligned} U_Y(\Theta_Y) &= \int_{-1/2w_0}^{1/2w_0} dy'\, e^{iy'\Theta_Y 2\pi/\lambda_1^{SH}} \\ &= (2w_0/\Theta_Y^*)\sin(\tfrac{1}{2}\Theta_Y^*), \end{aligned} \tag{19}$$

with

$$\Theta_Y^* = (2\pi w_0/\lambda_1^{SH})\Theta_Y\ ,$$

$$\begin{aligned} U_X(\Theta_X) &= \alpha_p 8(\pi)^{1/2}\frac{l^3\cos\theta_1^{SH}}{\lambda_2^{SH} w_0} \\ &\quad\times\left[\frac{2w_0}{\Theta_X^*}\sin(\tfrac{1}{2}W^*\Theta_X^*)\right]V(\Theta_X^*) \\ &\approx \alpha_r[(2w_0/\Theta_X^*)\sin(\tfrac{1}{2}\Theta_X)](w_0/\cos\theta_c)^{1/2}V(\Theta_X^*), \end{aligned} \tag{20}$$

where

$$V(\Theta_X^*) = (i)^{1/2}\{(\Theta_X^*)^{1/2}e^{-i/(4\Theta_X^*)}$$

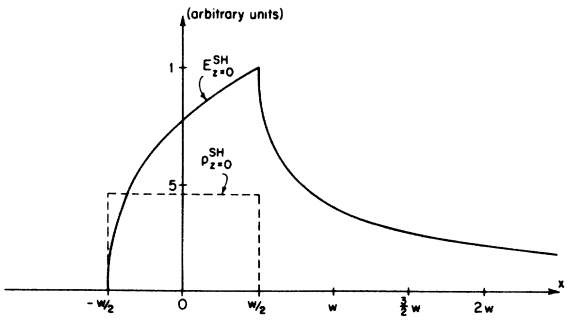

FIG. 5. Field distributions at the boundary of a nonlinear medium for the case of PMCTR. The fundamental field is assumed to have the rectangular shape given by the dotted line, and is incident from the left at the critical angle. The second-harmonic field along the boundary has the distribution given by the solid line.

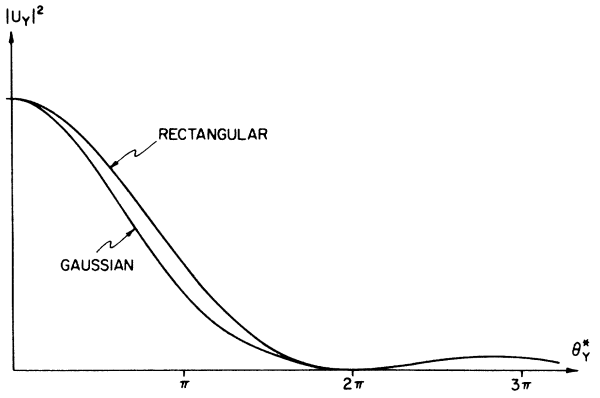

FIG. 6. Angular distribution of SH intensity in the far field in a direction normal to the plane of incidence. Angle Θ_Y^* is normalized to the diffraction limited angle $2\pi(w_0/\lambda_1^{SH})\Theta_Y$. The conventional diffraction patterns are valid for square and Gaussian distributions of the incident fundamental beam.

$$\times\ [1 - (1-i)\mathcal{E}_f(1/(2\pi\Theta_X^*)^{1/2})]$$

$$-\ (\Theta_X^*)^{1/2} + 1/(\pi i)^{1/2}\}, \tag{21}$$

$$W^* \approx 1,$$

$$\Theta_X^* \approx 2\pi(w_0/\lambda_1^{SH})\Theta_X\ ,$$

$$\alpha_r = 8(\pi\lambda_2^{SH})^{1/2}\alpha_p\ .$$

We have assumed small frequency dispersion for the indices of refraction in the above approximations.

Comparing Eq. (19) with Eq. (20), we see that aside from the factor α_r, the difference between the X and Y dependence of the far field is accounted for by $(w)^{1/2}V$. Since U_Y simply represents the well-known diffraction pattern from sharp edges, we may interpret the product $(w)^{1/2}V$ as the modification on the reflected SH diffraction pattern due to the phase match parallel to the boundary.

The squared amplitudes of U_Y and U_X are plotted in Figs. 6 and 7, respectively. It is seen that both V and U_Y are functions confined essentially to the regions near the origin Θ_X, $\Theta_Y \approx 0$. The former, however, has a sharper and narrower peak. The angular dependence of V therefore predominantly determines the form of U_X.

Whereas in all other cases the diffraction angle for the far field of the reflected SHG about is half the ratio of the SH wavelength to the beam width of the incident laser, i.e., $|\theta_d| \approx \lambda_1^{SH}/(2w_0)$, it becomes narrower for the special case of PMCTR. This is obvious from a comparison of Fig. 6 with Fig. 7. We may give a simple physical explanation as follows. From previous analysis for the case of PMCTR, it is clear that the reflected SH

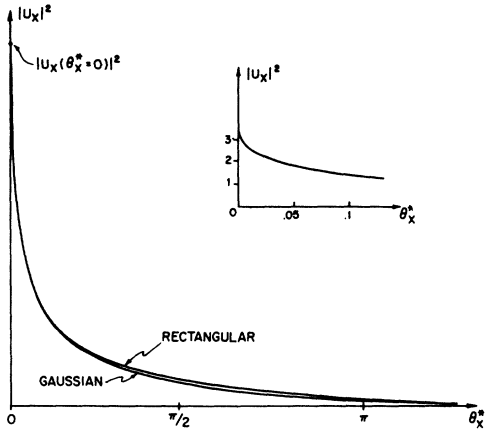

FIG. 7. Angular distribution of the SH intensity in the far field in the plane of incidence, as a function of the diffraction limited angle $\Theta_X^* = 2\pi(w_0/\lambda_1^{SH})\Theta_X$. Considerable narrowing occurs in the far field due to extended SH source distributions in the near field, both for the square and Gaussian distributions of the incident fundamental beam.

beam observed at the boundary has wider spread than the fundamental beam. In other words, it has an effective beam width larger than w_0. A narrower diffraction angle is thus expected on the basis of the uncertainty principle.

It is estimated by numerical evaluation that the half-power point of U_X is located at $\Theta_X^* \cong 0.5$. In other words, half of the reflected SH power is confined to $\Theta_X < \lambda_1^{SH}/(w_0 4\pi)$. Thus we conclude that we have a reduction of the diffraction angle by a factor of $(2\pi)^{-1}$ due to PMCTR.

Integrating $|U_X|^2$, $|U_Y|^2$ over all angles Θ_X, Θ_Y, we find the total integrated power in the case of PMCTR as

$$P_{PMCTR} = c(\lambda_0^{SH})^{-2} \int\int d\Theta_X d\Theta_Y \, |U_X U_Y|^2$$
$$\approx 64 \left(\frac{\pi^5}{2}\right)^{1/2} [cw_0^3/(\lambda_1^{SH}\cos\theta_1^{SH})] P_0^2$$
$$\times 2\int_0^\infty d\Theta_X^* \left| V e^{-(\Theta_X^*/4)^2} \right|^2$$
$$\approx 174.2 [cw_0^3/(\lambda_1^{SH}\cos\theta_1^{SH})] P_0^2 . \qquad (22)$$

This should be compared with the experimentally observed maximum shown in Fig. 2.

The integrated SH power is not simply proportional to the area of the incident beam w_0^2, but contains an extra factor w_0. This behavior may be understood on the basis of the effective penetration depth $l = (w_0\lambda/\cos\theta_c)^{1/2}$, introduced previously. In the phase-matched region the field at the boundary is proportional to $P_0^{SH} l$. This gives an extra factor w_0 in the SH power in PMCTR.

Numerical evaluation of Eq. (22) for the experimental conditions of Ref. 6, with an aperture with $w_0 = 0.3$ cm, shows that the SH power in PMCTR with an angle of incidence $\theta_i = 66.77°$ is larger by a factor 10^4 than this power away from the critical condition, where $\theta_i = 66°$. In this case the SH power may be evaluated with the simpler plane-wave theory. The present theory thus confirms the more qualitative theoretical considerations and the experimental results of Ref. 6.

IV. GOOS-HAENCHEN SHIFT IN HARMONIC GENERATION

As was already pointed out in the Introduction, a totally reflected beam of light undergoes a lateral displacement according to the laws of linear optics. In this section the nonlinear analog of this phenomenon will be considered. Qualitatively, two factors may be considered as contributing to the shift of reflected harmonic generation. One is caused by the displacement of the fundamental field inside the nonlinear medium, which causes a displacement D_L of the nonlinear source polarization. The other is the displacement D_{NL} of the reflected radiative field with the respect to this source, if the condition for total reflection for the second harmonic is met.

First, the nonlinear Goos-Haenchen shift will be examined for the case away from critical total reflection, i.e., away from singular points in $\vec{k}$ space. Then, the $\vec{k}$ space representation used in Ref. 5 is applicable, and the second-harmonic field at the interface may be expressed as

$$E_{z=0}^{SH} = (2\pi)^{-1} \int d\vec{k}_T \left(P^{SH}(\vec{k}_T)(2\omega/c)^2 \frac{(\vec{k}^S - \vec{k}^{SH})\cdot\hat{z}}{(\vec{k}_1^{SH} + \vec{k}^{SH})\cdot\hat{z}} \right.$$
$$\left. \times \frac{1}{(k^S)^2 - (k^{SH})^2} \right) . \qquad (23)$$

We have assumed that the crystal has a slight loss and is thick enough so that the effect due to the far end of the crystal is negligible.

The Fourier component of the nonlinear polarization is determined by the corresponding Fourier component of the square of the fundamental field inside the medium. If we restrict ourselves again to the case of E-field polarization perpendicular to the plane of incidence, the following relations hold:

$$P^{SH}(\vec{k}_T) = \chi_{eff} \tilde{E}_0^2 (\tilde{t}_{21})^2 , \qquad (24)$$

with

$$\tilde{E}_0^2 = \int\int E_0^2(x,y)_{z=0} e^{-i\vec{k}_T\cdot\vec{r}} dx dy \qquad (25)$$

and the convolution of the linear transmission factor with itself,

$$(\tilde{t}_{21})^2 = t_{21} \otimes t_{21} , \qquad (26)$$

$$t_{21} = 2\vec{k}_1 \cdot \hat{z} / [(\vec{k}_1 + \vec{k}_2)\cdot\hat{z}] . \qquad (27)$$

Substitution of Eqs. (24) and (25) into Eq. (23) yields the result

$$E^{SH}_{z=0} = (2\pi)^{-1} \int d\vec{k}_T \, \chi_{eff} \tilde{E}_0^2 F(\vec{k}_T) e^{i\vec{k}_T \cdot \vec{r}}, \tag{28}$$

where

$$F = (F^L \otimes F^L) F^{NL}, \qquad F^L = t_{21},$$

$$F^{NL} = t^{SH}_{21} \frac{(2\omega/c)}{2(\vec{k}^{SH} \cdot \hat{z})[(\vec{k}^{SH} + \vec{k}^S) \cdot \hat{z}]}$$

$$= \frac{(2\omega/c)^2}{(k^S)^2 - (k^{SH})^2} \frac{(\vec{k}^S - \vec{k}^{SH}) \cdot \hat{z}}{(\vec{k}_1^{SH} + \vec{k}^{SH}) \cdot \hat{z}}.$$

It is readily recognized that F^L and F^{NL} are related to the linear and the nonlinear Fresnel factors, respectively, which have been defined in the $\vec{k}$ space approach for the reflected SHG.[13]

Since the laser beam is well localized in the $\vec{k}$ space, $\tilde{E}_0^2$ is virtually zero except in the immediate vicinity of a fixed value of $\vec{k}_T$, namely, at $\vec{k}_T^0 = \vec{k}_2^0 \cdot (\overleftrightarrow{1} - \hat{z}\hat{z})$. To a good approximation, we may thus expand the factor F as follows:

$$F(\vec{k}_T) = F(\vec{k}_T^0) - i(\vec{k}_T' \cdot \vec{Q}) F(\vec{k}_T^0)$$

$$\cong F(\vec{k}_T^0) \exp[-i\vec{k}_T' \cdot \vec{Q}], \tag{29}$$

where

$$k_T' = \vec{k}_T - \vec{k}_T^0, \qquad \vec{Q} = -[F(\vec{k}_T^0)]^{-1} \left[\frac{\partial}{i\partial \vec{k}_T} F(\vec{k}_T) \right]_{k_T = k_T^0}.$$

It is valid provided F is analytic in the vicinity of $\vec{k}_T^0$.

Inserting Eq. (29) into Eq. (28), we conclude that

$$E^{SH}_{z=0} = \chi_{eff} F(\vec{k}_T^0) [E_0(\vec{r} - \vec{Q})]^2_{z=0} e^{i\vec{k}_T^0 \cdot \vec{r}}. \tag{30}$$

The implications of this expression are clear. The distribution of the SH field at the boundary plane is the same as that of the distribution of the square of the incident field, except for a lateral displacement equal to the real part of Q, and an additional phase distortion which depends on ImQ. The beam shift D may be written as

$$D = D^L + D^{NL} = \hat{x} \cdot \mathrm{Re}\vec{Q} \cos\theta_1^{SH}, \tag{31}$$

with

$$D^L = \mathrm{Im}\left(\frac{1}{F^L \cos\theta_1} \frac{\partial F^L}{\partial \theta_1} \right) \cos\theta_1^{SH}, \tag{32}$$

$$D^{NL} = \mathrm{Im}\left(\frac{1}{F^{NL} \cos\theta_1^{SH}} \frac{\partial F^{NL}}{\partial \theta_1} \right) \cos\theta_1^{SH}. \tag{33}$$

The technique described above is closely related to that employed by some authors[1,14] for the evaluation of the Goos-Haenchen shift in the linear case. There, the reflected beam was treated as consisting of two parts. The dominant part has the same beam shape as the incident light, whereas the other small part is related to the spatial derivative of the incident beam in the direction transverse to its propagation direction. In essence, this is equivalent to the Taylor series expansion to first order as expressed in Eq. (29). The dominant part obviously corresponds to the 0th-order term $F(\vec{k}_T^0)$. We may also easily identify the minor part there to the 1st-order term $(-i\vec{k}_T' \cdot \vec{Q}F)$ with the aid of the well-known theorem: If $f(x)$ has $\tilde{f}(k)$ as its Fourier transform then $ik\tilde{f}(k)$ is the transform of $d\tilde{f}(x)/dx$.

The total beam shift $D^L + D^{NL}$ may now be evaluated from Eqs. (28)–(33) in terms of the Goos-Haenchen shift in linear optics for perpendicular polarization of the beam,

$$D^L_{GH} = (\lambda_1/2\pi) \sin\theta_i (\sin^2\theta_i - \sin^2\theta_c)^{-1/2} \tag{34}$$

and in terms of a nonlinear shift, for total reflection of second-harmonic radiation,

$$D^{NL}_{GH} = (\lambda_1/4\pi) \sin\theta_k^{SH} (\sin^2\theta_i - \sin^2\theta_c^{SH})^{-1/2}. \tag{35}$$

Four cases must be distinguished:

(i) Neither beam is totally reflected; $D = 0$, since F^L and F^{NL} are both real.

(ii) Both beams are totally reflected,

$$D = D^L_{GH} \cos\theta^{SH}/2\cos\theta_i + D^{NL}_{GH}, \tag{36}$$

which occurs for $\theta_i > \theta_c$ and θ_c^{SH}.

(iii) The fundamental beam is totally reflected, but the second harmonic is not;

$$D = D^L_{GH} \left(\frac{\cos\theta_R^{SH}}{2\cos\theta_i} + \frac{\sin(\theta_R^{SH} + \theta_T^{SH})}{2\sin(\theta_i + \theta_c^{SH})} \right). \tag{37}$$

This situation occurs in a narrow range $\theta_c < \theta_i < \theta_c^{SH}$.

These three regimes have been realized in the experiments of Bloembergen, Simon, and Lee.[15] It is seen that total reflection of the fundamental beam contributes essentially a shift of the same

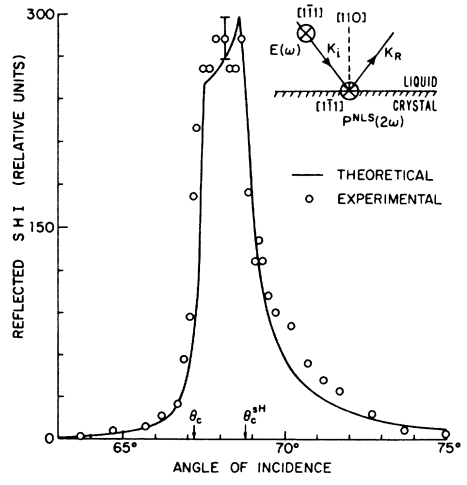

FIG. 8. Integrated second-harmonic power in reflection from a crystal of $NaClO_3$ as a function of the angle of incidence, according to Bloembergen, Simon, and Lee (Ref. 15). The drawn curve corresponds to the theory of Bloembergen and Pershan (Ref. 5). Cusplike behavior in the region around θ_c and θ_c^{SH} is evident.

order of magnitude as $\frac{1}{2}D_{GH}^{L}$, and so does total reflection of the second harmonic. The two contributions are additive. The experiments only observed the integrated SH in the far field, an example of which is reproduced in Fig. 8. The lateral displacement should, however, be experimentally observable

(iv) If the second harmonic met the condition for total reflection, but the fundamental field did not, which would occur for $\theta_c^{SH} < \theta_i < \theta_c$, the shift would be

$$D = D_{GH}^{NL} . \tag{38}$$

It is seen that Eqs. (32) and (33) for D_{GH}^{L} and D_{GH}^{NL} diverge as θ_i approaches θ_c or θ_c^{SH}, respectively. At the point of critical total reflection the function F is nonanalytic and the expansion (29) is not valid. The nonanalyticity is also apparent in the integrated reflected harmonic power curve, which according to Fig. 8 exhibits cusps at these points. Whereas the reflected field distribution has no singularity, the derivative does. The Green's-function technique of Sec. II can be employed to calculate the complete field distribution, and consequently the average shift, in the immediate vicinity of the critical points.

When the fundamental field only is critically reflected, Artman has already calculated the linear shift by a method, which is equivalent to our Green's-function procedure.[2]

He found for the shift near the critical angle for fundamental total reflection

$$D_{GH}^{L}(\theta_i = \theta_c) = (9/2\pi)\lambda_1 \cos\theta_c / \sin^2\theta_c . \tag{39}$$

Without going into detailed calculations, we may assume that this value should be used in Eqs. (36) and (37) for $\theta_i = \theta_c$. For critical SH total reflection the radiation pattern from a prescribed harmonic source polarization with effective penetration depth l may be calculated according to the methods of Sec. III. From Eqs. (2) and (7) it follows that the effective displacement is

$$D_{GH}^{NL}(\theta_i = \theta_c^{SH}) = \frac{4\pi}{\lambda_2^{SH}} l^2 . \tag{40}$$

If the fundamental is already totally reflected $\theta_c < \theta_c^{SH}$, the effective penetration depth for the source is

$$l = \frac{\lambda_1}{4\pi} (\sin^2\theta_c^{SH} - \sin^2\theta_c)^{-1/2} . \tag{41}$$

The second-harmonic displacement is increased significantly, but does not diverge, as Eq. (33) would indicate.

For phase matching the two critical angles coalesce, $\theta_c = \theta_c^{SH}$. In this case Eq. (41) also diverges and one must return to the direct calculation of the radiation pattern in Sec. III for PMCTR.

Note that, according to Eq. (41), the effective penetration depth l is proportional to the square root of the product of the coherence length l_{coh} and the wavelength as previously predicted by Bloembergen and Lee[6] and discussed by Shih.[11]

It is clear from Fig. 5 that the net average displacement of the beam pattern in the near field becomes a significant fraction of the width w_0 of the incident beam. The "center of the gravity" of the square beam is in fact shifted by $0.36w_0$ from the center of the incident beam, which was assumed to have a rectangular shape. In this case both the beam distortion and displacement are maximum.

V. CONCLUSIONS

An observable lateral displacement is predicted for second-harmonic generation in situations of total reflection. This is the nonlinear analog of the Goos-Haenchen shift. A diffraction theory has been given for the case of phase-matched critical total reflection, in which case the behavior of the parametrically reflected light depends sensitively on the lateral dimension of the incident fundamental beam. In this case the SH lateral displacement becomes comparable to the beam width.

---

*Research supported in part by the Joint Services Electronics Program, under Contract No. N00014-67-A-0298-0006.

†Vinson Hayes Senior Fellow.

[1]For a good collection of the references on the linear Goos-Haenchen shift, see, for example, H. Lotsch, J. Opt. Soc. Am. 58, 551 (1968).

[2]K. Artman, Ann. Physik 8, 270 (1951).

[3]F. Goos and H. Haenchen, Ann. Physik 1, 333 (1947).

[4]F. Goos and H. Lindberg-Haenchen, Ann. Physik 5, 251 (1949).

[5]N. Bloembergen and P. S. Pershan, Phys. Rev. 128, 606 (1962).

[6]N. Bloembergen and C. H. Lee, Phys. Rev. Letters 19, 835 (1967).

[7]P. P. Bey, J. F. Giuliani, and H. Rabin, Phys. Rev. 184, 849 (1969).

[8]G. D. Boyd, A. Ashkin, J. M. Dziedzic, and D. A. Kleinman, Phys. Rev. 137, 1305 (1965).

[9]D. A. Kleinman, A. Ashkin, and G. D. Boyd, Phys. Rev. 145, 3381 (1966).

[10]H. Shih and N. Bloembergen, Phys. Rev. 184, 895 (1969).

[11]H. Shih, Ph. D. thesis, Harvard University, 1970 (unpublished). This references gives more details of the calculation.

[12]M. Born and E. Wolf, *Principle of Optics* (Pergamon, New York, 1966), 3rd ed., Chap. VIII.

[13]The nonlinear Fresnel factor F^{NL} is identical to Eq. (4.4) of Ref. 5. Our notation $\hat{k}^S$, $\hat{k}^{SH}$, $\hat{k}_1^{SH}$ correspond, respectively, to $\hat{k}^S(2\omega)$, $\hat{k}^T(2\omega)$, and $\hat{k}^R(2\omega)$ in Ref. 5.

[14]C. Schaefer and R. Pich, Ann. Physik 30, 245 (1937).

[15]N. Bloembergen, J. Simon, and C. H. Lee, Phys. Rev. 181, 1261 (1969).